



ORIGINAL ARTICLE

# Effects of heat source/sink and induced magnetic field on natural convective flow in vertical concentric annuli



Dileep Kumar \*, A.K. Singh

Department of Mathematics, Institute of Science, Banaras Hindu University, Varanasi 221005, India

Received 9 February 2016; revised 2 July 2016; accepted 25 August 2016

Available online 16 September 2016

## KEYWORDS

Natural convection;  
Heat source/sink;  
Induced magnetic field;  
Skin-friction;  
Nusselt number;  
Magnetohydrodynamics

**Abstract** In the present analysis, we have investigated the effects of induced magnetic field and heat source/sink on fully developed laminar natural convective flow of a viscous incompressible and electrically conducting fluid in the presence of radial magnetic field by considering induced magnetic field into account. The governing equations of the considered model are transformed into simultaneously ordinary differential equations and solved analytically. We have analyzed the effect of Hartmann number, heat source/sink parameter and ratio of outer radius to inner radius on the fluid velocity, induced magnetic field, induced current density and temperature field by the graphs while the values of skin-friction, Nusselt number, mass flux and induced current flux are given in the tabular form. We observed that the values of the velocity, induced magnetic field and induced current density have decreasing tendency with increasing the values of the Hartmann number. The results show that an increasing value of the heat source/sink parameter leads to increase the velocity, induced magnetic field, induced current density and temperature in case of heat source and vice versa in case of heat sink.

© 2016 Faculty of Engineering, Alexandria University. Production and hosting by Elsevier B.V. This is an open access article under the CC BY-NC-ND license (<http://creativecommons.org/licenses/by-nc-nd/4.0/>).

## 1. Introduction

The studies of natural convective flow along a vertical cylinder have wider range of applications in so many fields such as technology, agriculture, oceanography and geothermal power generation. The study of transport phenomenon with annular geometry has attracted its applications in the thermal recovery

of oil, solar power collectors and design of magnetohydrodynamic power generators, etc. The magnetohydrodynamics may be used for pinching the hot plasma. In oceanography, the speed of ships is measured by MHD flow meter in which the induced voltage is proportional to the flow rate. We can optimize the fluid flow by using heat source/sink in concentric annulus. The flow of viscous incompressible fluid in concentric annuli was first studied by Couette [1] in order to measure the fluid viscosity. Some authors, such as Ramamoorthy [2], Jain and Mehta [3], Raptis and Singh [4], Chamkha [5], Jha and Apere [6], Sheikholeslami et al. [7,8,11,12], Hamza et al. [9], and Sheikholeslami and Rashidi [10] have studied the MHD flow problems with neglecting the induced magnetic field.

\* Corresponding author.

E-mail addresses: [dileepyadav02april@gmail.com](mailto:dileepyadav02april@gmail.com) (D. Kumar), [ashok@bhu.ac.in](mailto:ashok@bhu.ac.in) (A.K. Singh).

Peer review under responsibility of Faculty of Engineering, Alexandria University.

<http://dx.doi.org/10.1016/j.aej.2016.08.019>

1110-0168 © 2016 Faculty of Engineering, Alexandria University. Production and hosting by Elsevier B.V.

This is an open access article under the CC BY-NC-ND license (<http://creativecommons.org/licenses/by-nc-nd/4.0/>).

**Nomenclature**

$a$	radius of inner cylinder	$u'$	velocity of fluid along axial direction
$b$	radius of outer cylinder	$U$	characteristics velocity of fluid
$g$	acceleration due to gravity	$Nu_1$	Nusselt number at inner cylinder
$H'_0$	constant magnetic field	$Nu_\lambda$	Nusselt number at outer cylinder
$H'_z$	induced magnetic field in $z'$ -direction	$Q_0$	volumetric rate of heat generation/absorption
$H$	non-dimensional induced magnetic field in $z$ -direction	$S$	heat source/sink parameter
$C_p$	specific heat at constant pressure	<i>Greek symbols</i>	
$J_\theta$	induced current density long $\theta$ -direction	$\beta$	coefficient of thermal expansion
Ha	Hartmann number	$\kappa$	thermal conductivity of the fluid
$r', \theta', z'$	cylindrical coordinates	$\mu_e$	magnetic permeability
$r$	non-dimensional radial distance	$\nu$	kinematic viscosity of the fluid
$T'$	temperature of the fluid	$\eta$	magnetic diffusivity
$T$	temperature of the fluid in non-dimensional form	$\rho$	density of the fluid
$T'_f$	ambient temperature	$\lambda$	ratio of outer radius and inner radius
$T'_w$	temperature at outer surface of inner cylinder	$\sigma$	conductivity of the fluid
$u$	fluid velocity in non-dimensional form along axial direction	$\tau_1$	skin friction coefficient at inner cylinder
		$\tau_\lambda$	skin friction coefficient at outer cylinder

Arora and Gupta [13] have extended the Jain and Mehta's problem with considering the effect of induced magnetic field. The analytical solutions for the fully developed natural convection in open ended vertical concentric annuli with mixed kind of thermal boundary conditions under a radial magnetic field have been obtained by Singh et al. [14]. Guria et al. [15] have performed the study of effects of wall conductance on MHD fully developed flow with asymmetric heating of the wall. Singh et al. [16] have studied the hydromagnetic free convection in the presence of induced magnetic field. Later on, the effect of induced magnetic field on natural convection in vertical concentric annuli has been investigated by Singh and Singh [17]. Further, Kumar and Singh [18] have discussed the effect of the induced magnetic field on free convection when the concentric cylinders are heated/cooled asymmetrically.

In many problems, there may be plausible temperature difference between the surface and the ambient fluid. This obligates the consideration of temperature dependent heat sources/sinks which may exert strong effect on the heat transfer characteristics. The study of heat source/sink in MHD fluid flow is gaining attention because of its increasing application to many engineering problems. The application of heat transfer is very significant in production engineering to improve the quality of the final product. The flow over a stretching plate was first considered by Crane [19] who found a closed form of analytic solution of the self-similar equation for steady boundary layer flow of a Newtonian fluid. The mixed convection flow over a vertical plate with localized heating and cooling along with magnetic effects and suction/injection effects was studied by Chamkha et al. [20]. Sharma and Singh [21] investigated the effect of variable thermal conductivity and heat source/sink on MHD flow near a stagnation point on a linear stretching sheet. Recently, Bhattacharyya [22] analyzed the effects of heat source/sink on MHD flow and heat transfer over a shrinking sheet with mass suction. Lavanya and Ratnam [23] have obtained analytical solution by taking the effect of radiation and mass transfer on unsteady MHD natural convective flow

past a vertical porous plate embedded in a porous medium in a slip flow regime with heat source/sink and Soret effect. Babu et al. [24] have studied the effects of radiation and heat source/sink on the steady two dimensional magnetohydrodynamic (MHD) boundary layer flow past a shrinking sheet with wall mass suction by numerical technique. Ibrahim et al. [25] have obtained the numerical solution of effects of variable thermal conductivity and heat generation on the flow of a viscous incompressible and electrically conducting fluid in the presence of a uniform transverse magnetic field with variable free stream near a stagnation point on a non-conducting stretching sheet. Recently, Kumar and Singh [26] have studied the exact analysis of effects of Newtonian heating/cooling and induced magnetic field on natural convective flow in an annulus cylinders.

Here, the aim was to discuss the effects of heat source/sink and induced magnetic field on natural convective flow in vertical concentric annuli with radial magnetic field. We have obtained the analytical solution for the velocity, induced magnetic field and temperature field by solving the non-dimensional governing linear simultaneous ordinary differential equations using the non-dimensional boundary condition. Also, we have obtained the analytical solution for the governing differential equations at singular point  $Ha = 2.0$ . Finally, we focus on the effects of the heat source/sink parameter and the Hartmann number on the velocity, induced magnetic, induced current density, Nusselt number, skin-friction, mass flux and induced current flux using graphs and tables. We can compare this analysis with Singh and Singh [17] by taking  $S = 0$ , i.e. in the absence of heat source/sink.

## 2. Mathematical formulation

The governing equations of an electrically conducting fluid in hydromagnetic flow together with the Maxwell's electromagnetic equations in the steady state case are as follows:

**Continuity equation**

$$\nabla \cdot \mathbf{V} = 0, \quad (1)$$

**Momentum equation**

$$\rho(\mathbf{V} \cdot \nabla)\mathbf{V} = -\nabla P + \mu(\nabla^2 \mathbf{V}) + (\mathbf{J} \times \mathbf{B}) + \rho \mathbf{g}, \quad (2)$$

**Magnetic field equation**

$$(\nabla^2 \mathbf{H}) + \nabla \times (\mathbf{V} \times \mathbf{H}) = 0, \quad (3)$$

**Energy equation**

$$(\mathbf{V} \cdot \nabla)T = \frac{\kappa}{\rho C_p} \nabla^2 T + \frac{Q_0}{\rho C_p}. \quad (4)$$

We have considered the steady and laminar flow of a viscous, incompressible and electrically conducting fluid in the fully developed region between vertical concentric annuli of infinite length with heat source/sink and induced magnetic field. The  $z'$ -axis is taken along the axis of the co-axial cylinders and measured in the vertical upward direction and  $r'$ -denotes the radial direction measured outward from the axis of cylinder. Also the applied magnetic field is directed radially outward in the form of  $[aH'_0/r']$ . The radius of inner and outer cylinders is taken as  $a$  and  $b$  respectively. We take  $T'_w$  and  $T'_f$  the temperatures at outer surface of inner cylinder and the ambient temperature respectively. Let  $z'$  be the direction of the flow along the axis of concentric cylinders. Therefore, the radial and tangential components of the velocity are taken as zero i.e.  $u'_{r'} = u'_{\theta'} = 0$ . The velocity component  $u'_{z'}$  is independent of  $\theta'$  due to axial symmetry of fluid flow. The transport phenomena depend only on the variable  $r'$  because the flow of fluid is fully developed and the cylinders are of infinite length. So, for the considered model the velocity and magnetic fields are given by  $[0, 0, u'(r')]$  and  $[aH'_0/r', 0, H'_z(r')]$  respectively.

As components of  $\mathbf{H}$  and  $\mathbf{V}$  are  $[0, 0, u'(r')]$  and  $[aH'_0/r', 0, H'_z(r')]$  respectively, we have (see Fig. 1)

$$\begin{aligned} \nabla^2 \mathbf{V} &= \left\{ \frac{1}{r'} \frac{\partial}{\partial r'} \left( r' \frac{\partial \mathbf{V}}{\partial r'} \right) + \frac{1}{r'^2} \frac{\partial^2 \mathbf{V}}{\partial \theta'^2} + \frac{\partial^2 \mathbf{V}}{\partial z'^2} \right\} \\ &= \left\{ \frac{1}{r'} \frac{\partial}{\partial r'} \left( r' \frac{\partial \mathbf{V}}{\partial r'} \right) \right\} = \left\{ \frac{d^2 u'}{dr'^2} + \frac{1}{r'} \frac{du'}{dr'} \right\}, \end{aligned} \quad (5)$$

$$\nabla^2 \mathbf{H} = \left\{ \frac{d^2 H'_z}{dr'^2} + \frac{1}{r'} \frac{dH'_z}{dr'} \right\}, \quad (6)$$

$$\mathbf{J} \times \mathbf{B} = (\nabla \times \mathbf{H}) \times \mathbf{B} = \mu_e (\nabla \times \mathbf{H}) \times \mathbf{H} = \frac{a\mu_e H'_0}{r'} \frac{dH'_z}{dr'}, \quad (7)$$

$$\nabla \times (\mathbf{V} \times \mathbf{H}) = \frac{aH'_0}{r'} \frac{du'}{dr'}. \quad (8)$$

Using Eqs. (5)–(8) in Eqs. (1)–(4), the basic transport equations for the considered model by applying the Boussinesq approximation are obtained as follows [17]:

$$v \left( \frac{d^2 u'}{dr'^2} + \frac{1}{r'} \frac{du'}{dr'} \right) + g\beta(T' - T'_f) + \frac{a\mu_e H'_0}{\rho r'} \frac{dH'_z}{dr'} = 0, \quad (9)$$

$$\eta \left( \frac{d^2 H'_z}{dr'^2} + \frac{1}{r'} \frac{dH'_z}{dr'} \right) + \frac{aH'_0}{r'} \frac{du'}{dr'} = 0, \quad (10)$$

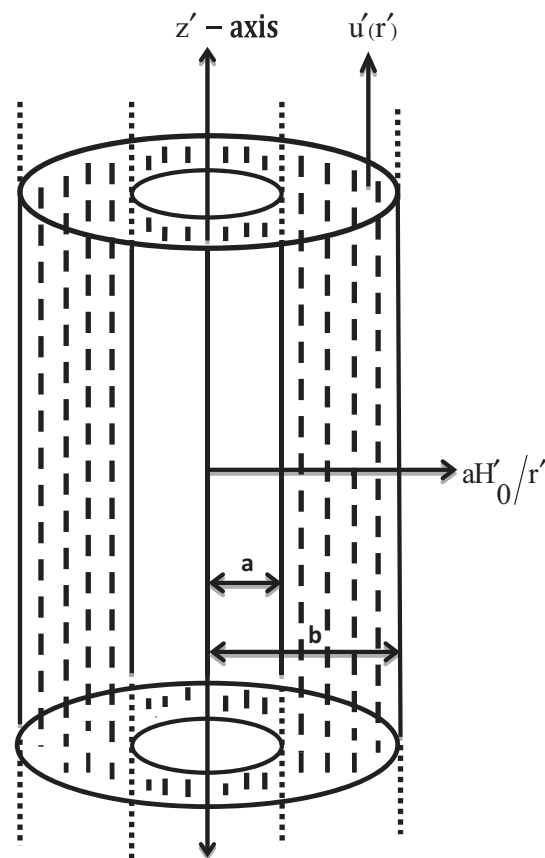


Figure 1 Physical model.

$$\frac{\kappa}{\rho C_p} \left( \frac{d^2 T'}{dr'^2} + \frac{1}{r'} \frac{dT'}{dr'} \right) + \frac{Q_0}{\rho C_p} = 0. \quad (11)$$

The boundary conditions for the velocity, induced magnetic field and temperature field are given as follows:

$$u' = H'_z = 0, \quad T' = T'_w, \quad \text{at } r' = a, \quad (12)$$

$$u' = H'_z = 0, \quad T' = T'_f, \quad \text{at } r' = b. \quad (13)$$

in the above equations,  $u'$ ,  $g$ ,  $\beta$ ,  $\mu_e$ ,  $\rho$ ,  $\eta$ ,  $\kappa$ ,  $C_p$ ,  $T'$ ,  $T'_f$  and  $Q_0$  are the fluid velocity, acceleration due to gravity, coefficient of volume expansion, magnetic permeability, density of the fluid, magnetic diffusivity, thermal conductivity of the fluid, specific heat at constant pressure, temperature of the fluid, ambient temperature and heat source for  $Q_0 > 0$  and heat sink for  $Q_0 < 0$  respectively.

Application of the non-dimensional variables defined as

$$\begin{aligned} u &= u'/U, \quad r = r'/a, \quad \lambda = b/a, \quad T = (T' - T'_f)/(T'_w - T'_f), \\ H &= (H'_z)/(\sigma a \mu_e H'_0 U), \end{aligned} \quad (14)$$

in Eqs. (9)–(11) has resulted the following equations in non-dimensional form:

$$\frac{d^2 u}{dr^2} + \frac{1}{r} \frac{du}{dr} + \frac{\text{Ha}^2}{r} \frac{dH}{dr} + T = 0, \quad (15)$$

$$\frac{d^2 H}{dr^2} + \frac{1}{r} \frac{dH}{dr} + \frac{1}{r} \frac{du}{dr} = 0, \quad (16)$$

$$\frac{d^2 T}{dr^2} + \frac{1}{r} \frac{dT}{dr} + S = 0. \quad (17)$$

The boundary conditions for the velocity, induced magnetic field and temperature field in non-dimensional form are obtained as follows:

$$u = H = 0, \quad T = 1, \quad \text{at } r = 1, \quad (18)$$

$$u = H = 0, \quad T = 0, \quad \text{at } r = \lambda. \quad (19)$$

In above equations, we have used some additional non-dimensional parameters such as the Hartmann number, the heat source/sink parameter and characteristic velocity of the fluid and they are defined as follows:

$$\begin{aligned} \text{Ha} &= \mu_e a H'_0 \sqrt{\sigma/\mu}, \quad U = g\beta a^2 (T'_w - T'_f)/\nu, \\ S &= Q_0/\kappa(T'_w - T'_f) = (Q_0 a^4 g\beta)/\kappa(U\nu). \end{aligned} \quad (20)$$

### 3. Analytical solution

#### 3.1. Solution for Hartmann number (Ha) $\neq$ 2.0 & 4.0

Analytical solutions of Eqs. (15)–(17) with boundary conditions (18) and (19) are obtained as follows:

$$u = A_1 r^{\text{Ha}} + A_2 r^{-\text{Ha}} + A_3 + (A_4 \log r + A_5) r^2 + A_6 S r^4, \quad (21)$$

$$H = A_7 - (A_1 r^{\text{Ha}} - A_2 r^{-\text{Ha}})/\text{Ha} + r^2 \{A_4(1 - 2 \log r) - 2A_5\} / 4 - (A_6 S r^4)/4, \quad (22)$$

$$T = A_8 + A_9 \log r - S r^2/4. \quad (23)$$

The skin-frictions and the Nusselt number at outer surface of inner cylinder and at inner surface of outer cylinder in non-dimensional form are obtained by using Eqs. (21) and (23) as follows:

$$\tau_1 = \left( \frac{du}{dr} \right)_{r=1} = \text{Ha}(A_1 - A_2) + (A_4 + 2A_5) + 4A_6 S, \quad (24)$$

$$\begin{aligned} \tau_\lambda &= - \left( \frac{du}{dr} \right)_{r=\lambda} \\ &= \text{Ha}(A_2 \lambda^{-\text{Ha}-1} - A_1 \lambda^{\text{Ha}-1}) - \{A_4(1 + 2 \log \lambda) + 2A_5\} \lambda \\ &\quad - 4A_6 S \lambda^3, \end{aligned} \quad (25)$$

$$Nu_1 = - \left( \frac{dT}{dr} \right)_{r=1} = -(A_9 - S/2), \quad (26)$$

$$Nu_\lambda = - \left( \frac{dT}{dr} \right)_{r=\lambda} = -(A_9/\lambda - S\lambda/2). \quad (27)$$

The induced current density along  $\theta$ -direction is obtained by Maxwell's equation as follows:

$$\begin{aligned} J_\theta &= - \left( \frac{dH}{dr} \right) \\ &= A_1 r^{\text{Ha}-1} + A_2 r^{-\text{Ha}-1} + (A_4 \log r + A_5) r + A_6 S r^3. \end{aligned} \quad (28)$$

The mass flux and the induced current flux of the fluid through the annuli are obtained by using Eqs. (21) and (22) as follows:

$$\begin{aligned} Q &= 2\pi \int_1^\lambda r u dr \\ &= 2\pi [A_1 (\lambda^{\text{Ha}+2} - 1)/(\text{Ha} + 2) + A_2 (\lambda^{-\text{Ha}+2} - 1)/(-\text{Ha} + 2) \\ &\quad + A_3 (\lambda^2 - 1)/2 + A_4 \{\lambda^4 (4 \log \lambda - 1) + 1\}/16 \\ &\quad + A_5 (\lambda^4 - 1)/4 + A_6 S (\lambda^6 - 1)/6], \end{aligned} \quad (29)$$

$$\begin{aligned} J &= \{A_1 (\lambda^{\text{Ha}} - 1) - A_2 (\lambda^{-\text{Ha}} - 1)\}/\text{Ha} + A_4 \{2\lambda^2 \log \lambda \\ &\quad - (\lambda^2 - 1)\}/4 + A_5 (\lambda^2 - 1)/2 + A_6 S (\lambda^4 - 1)/4. \end{aligned} \quad (30)$$

The constants  $A_1, A_2, A_3, A_4, A_5, A_6, A_7, A_8$  and  $A_9$  appearing in above equations are defined in [Appendix A](#).

#### 3.2. Solution for Hartmann number (Ha) = 2.0

In this section, we have solved the governing differential equations for the singular point  $\text{Ha} = 2.0$  because the mathematical expressions  $A_4 = \{-A_9/(4 - \text{Ha}^2)\}$  and  $A_5 = \{4A_9/(4 - \text{Ha}^2)^2 - A_8/(4 - \text{Ha}^2)\}$  occurring in Eqs. (21) and (22) clearly indicate that they have the singularity at  $\text{Ha} = 2.0$ . The expressions for the velocity and induced magnetic field at  $\text{Ha} = 2.0$  are given as follows:

$$u = B_1 r^2 + B_2 r^{-2} + B_3 + r^2 \log r (B_4 \log r + B_5) + B_6 S r^4, \quad (31)$$

$$\begin{aligned} H &= B_7 - (B_1 r^2 - B_2 r^{-2})/2 + r^2 \{B_8 + (B_9 + B_{10} \log r) \log r\} \\ &\quad + B_{11} S r^4. \end{aligned} \quad (32)$$

In this case, the skin-friction at cylindrical walls and induced current density along  $\theta$ -direction are obtained as follows:

$$\tau_1 = 2(B_1 - B_2) + B_5 + 4B_6 S, \quad (33)$$

$$\begin{aligned} \tau_\lambda &= -2(B_1 \lambda - B_2 \lambda^{-3}) - \lambda \{2(B_4 + B_5) \log \lambda \\ &\quad + 2B_4 (\log \lambda)^2 + B_5\} - 4B_6 S \lambda^3, \end{aligned} \quad (34)$$

$$J_\theta = B_1 r + B_2 r^{-3} + r \log r (B_4 \log r + B_5) + B_6 S r^3. \quad (35)$$

Also, in this case the mass flux and induced current flux are given as follows:

$$\begin{aligned} Q &= 2\pi [B_1 (\lambda^4 - 1)/4 + B_2 \log \lambda + B_3 (\lambda^2 - 1)/2 + \{8B_4 \lambda^4 (\log \lambda)^2 \\ &\quad + 2(B_5 - 2B_4) \lambda^4 \log \lambda + 8(B_4 - B_5)\}/32 \\ &\quad + B_6 S (\lambda^6 - 1)/6], \end{aligned} \quad (36)$$

$$\begin{aligned} J &= [\{B_1 (\lambda^2 - 1) - B_2 (\lambda^{-2} - 1)\}/2 + A_6 S (\lambda^4 - 1)/4 \\ &\quad + \{2B_4 \lambda^2 (\log \lambda)^2 + 2(B_5 - B_4) \lambda^2 \log \lambda - (B_4 + B_5) \\ &\quad \times (\lambda^2 - 1)\}/4]. \end{aligned} \quad (37)$$

The constants  $B_1, B_2, B_3, B_4, B_5, B_6, B_7, B_8, B_9, B_{10}$  and  $B_{11}$  occurring in above equations are defined in [Appendix B](#).

#### 3.3. Solution for Hartmann number (Ha) = 4.0

Here, we have calculated the expression for the velocity and induced magnetic field at another singular point  $\text{Ha} = 4.0$  because the mathematical expression  $A_6 = \{1/4(16 - \text{Ha}^2)\}$  appearing in Eqs. (21) and (22). The solution for  $u$  and  $H$  at  $\text{Ha} = 4.0$  is as follows:

$$u = C_1 r^4 + C_2 r^{-4} + C_3 + r^2(C_4 \log r + C_5) + C_6 S r^4 \log r, \quad (38)$$

$$H = C_7 - (C_1 r^4 - C_2 r^{-4})/4 + r^2(C_8 + C_9 \log r) + (C_{10} + C_{11} \log r) S r^4. \quad (39)$$

The skin-friction at cylindrical walls and induced current density along  $\theta$ -direction are calculated in this case as follows:

$$\tau_1 = 4(C_1 - C_2) + C_4 + 2C_5 + 4C_6 S, \quad (40)$$

$$\tau_\lambda = -4(C_1 \lambda^3 - C_2 \lambda^{-5}) - \lambda(C_4 + 2C_5 + 2C_6 \log \lambda) - C_6 S \lambda^3 (4 \log \lambda + 1), \quad (41)$$

$$J_\theta = C_1 r^3 + C_2 r^{-5} + r(C_4 \log r + C_5) + C_6 S r^3 \log r. \quad (42)$$

The mass flux and induced current flux for singular point  $Ha = 4.0$  are obtained as follows:

$$Q = 2\pi[C_1(\lambda^6 - 1)/6 - C_2(\lambda^{-2} - 1)/2 + C_3(\lambda^2 - 1)/2 + \{4C_4 \lambda^4 \log \lambda + (4C_5 - C_4)(\lambda^4 - 1)\}/16 + B_6 S \{6\lambda^6 \log \lambda - (\lambda^6 - 1)\}/36], \quad (43)$$

$$J = [\{C_1(\lambda^4 - 1) - C_2(\lambda^{-4} - 1)\}/4 + \{2C_4 \lambda^2 \log \lambda + (2C_5 - C_4)(\lambda^2 - 1)\}/4 + A_6 S \{4\lambda^4 \log \lambda - (\lambda^4 - 1)\}/16]. \quad (44)$$

The constants  $C_1, C_2, C_3, C_4, C_5, C_6, C_7, C_8, C_9, C_{10}, C_{11}$  and  $C_{12}$  are defined in [Appendix C](#).

### 4. Results and discussion

The effects of heat source/sink parameter, Hartmann number and ratio of outer radius to inner radius on the velocity of the fluid are shown in [Figs. 2a–2c](#). Observation of [Figs. 2a](#)

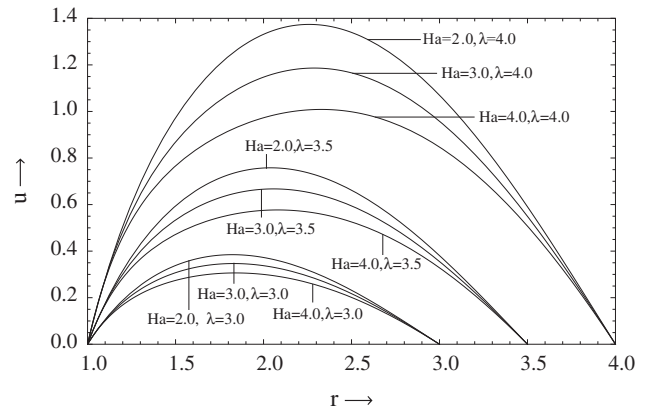


**Figure 2c** Effect of the ratio of outer radius to inner radius on the velocity profiles with  $Ha = 2.0, 3.0, 4.0$  at  $S = 1.0$ .

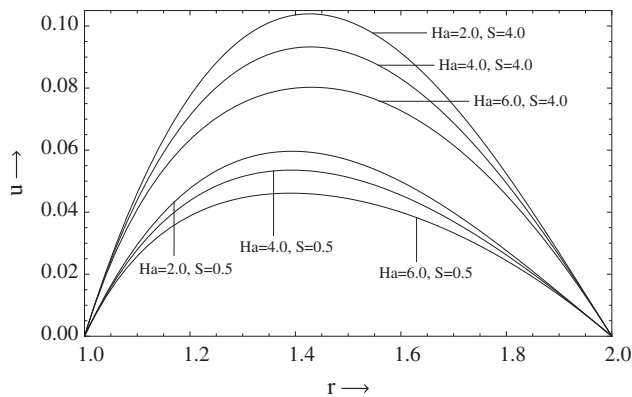


**Figure 2a** Effect of the heat source/sink parameter ( $S = 0.5, 4.0$ ) on the velocity profiles with  $Ha = 2.0, 4.0, 6.0$  at  $\lambda = 2.0$ .

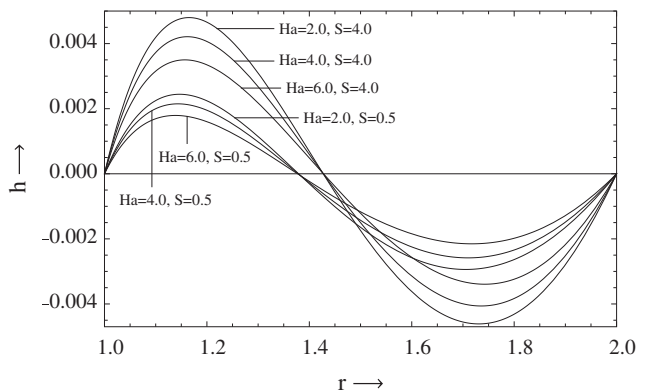


**Figure 3a** Effect of the heat source/sink parameter ( $S = 0.5, 4.0$ ) on the induced magnetic field profiles with  $Ha = 2.0, 4.0, 6.0$  at  $\lambda = 2.0$ .

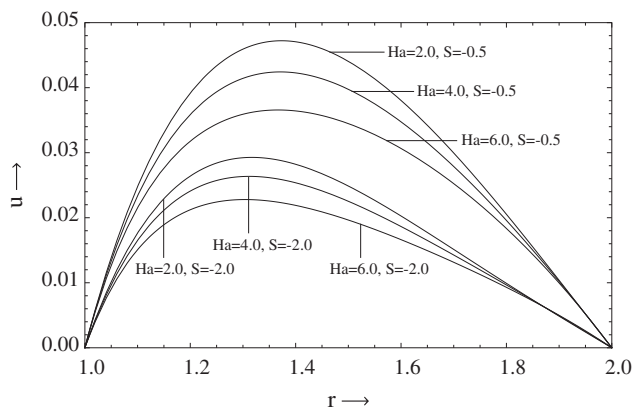


**Figure 2b** Effect of the heat source/sink parameter ( $S = -0.5, -2.0$ ) on the velocity profiles with  $Ha = 2.0, 4.0, 6.0$  at  $\lambda = 2.0$ .

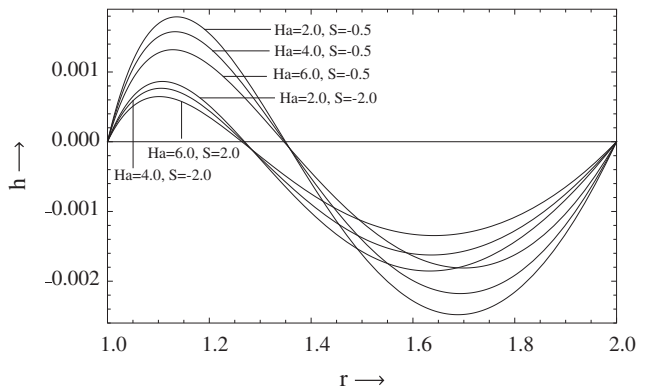


**Figure 3b** Effect of the heat source/sink parameter ( $S = -0.5, -2.0$ ) on the induced magnetic field profiles with  $Ha = 2.0, 4.0, 6.0$  at  $\lambda = 2.0$ .

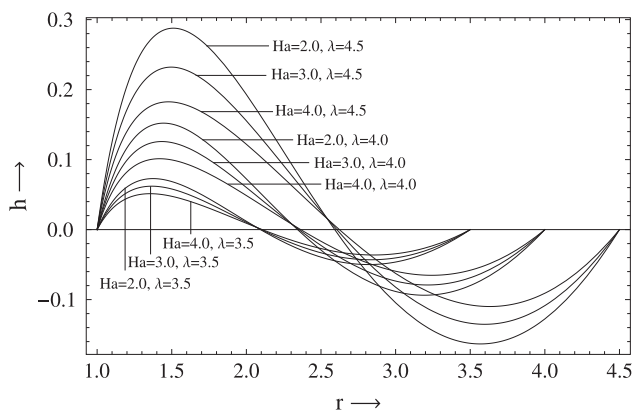


**Figure 3c** Effect of the ratio of outer radius to inner radius on the induced magnetic field with  $Ha = 2.0, 3.0, 4.0$  at  $S = 1.0$ .

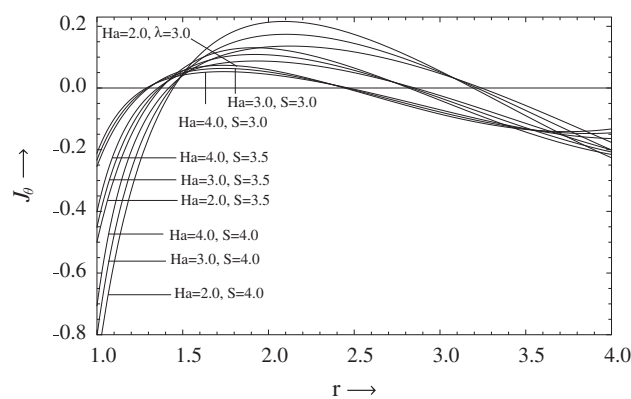


**Figure 4c** Effect of the ratio of outer radius to inner radius on the induced current density field profiles with  $Ha = 2.0, 3.0, 4.0$  at  $S = 1.0$ .

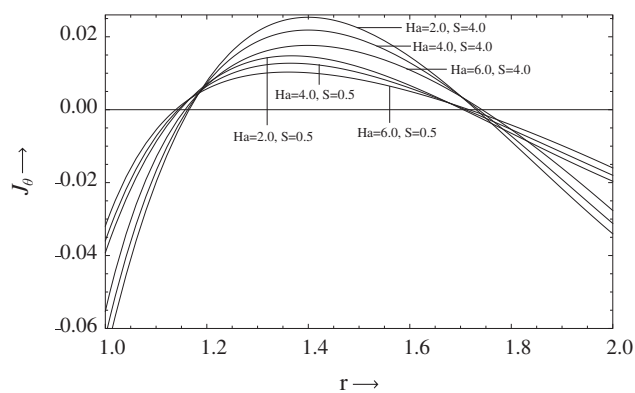


**Figure 4a** Effect of the heat source/sink parameter ( $S = 0.5, 4.0$ ) on the induced current density field profiles with  $Ha = 2.0, 3.0, 4.0$  at  $\lambda = 2.0$ .

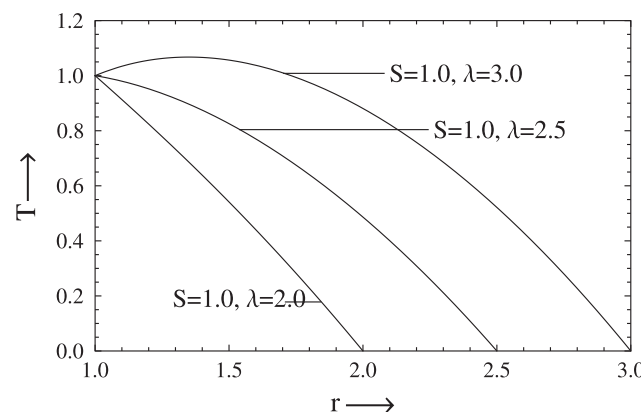


**Figure 5a** Effect of the ratio of outer radius to inner radius on the temperature field at  $S = 1.0$ .

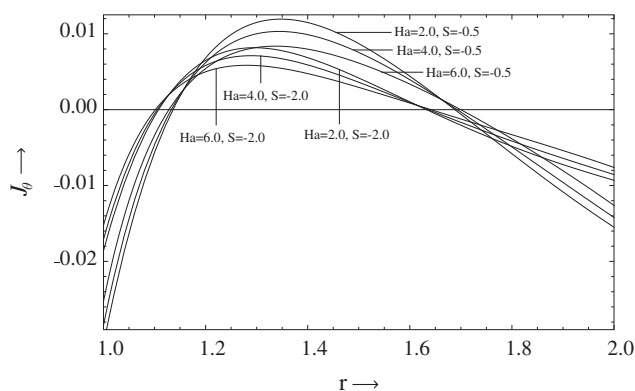


**Figure 4b** Effect of the heat source/sink parameter ( $S = -0.5, -2.0$ ) on the induced current density field profiles with  $Ha = 2.0, 3.0, 4.0$  at  $\lambda = 2.0$ .

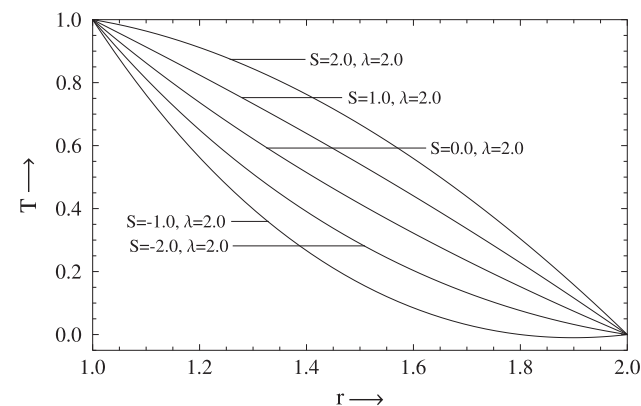


**Figure 5b** Effect of the heat source/sink parameter on the temperature field at  $\lambda = 2.0$ .

and 2b clearly indicates that with increasing value of the heat source/sink parameter, fluid velocity increases in the case of heat source and decreases in the case of heat sink because the thickness of thermal boundary layer enhances (internal heat energy increases) in case of increasing heat source parameter and reduces (internal heat energy decreases) in case of

increasing heat sink parameter. Also, it is clear from Figs. 2a and 2b that the velocity decreases in both cases (heat source and heat sink) with increasing value of the Hartmann number because the Lorentz forces increases with increasing the Hartmann number. The presence of Lorentz force reduces the force on the velocity field and hence the velocity profile

**Table 1** Numerical values of the Nusselt number at inner and outer cylinder in non-dimensional form.

$S$	$\lambda$	$Nu_1$	$Nu_2$
-2.0	2.0	2.60674	-0.196631
	3.0	3.55120	-1.482930
-1.0	2.0	2.02472	0.262358
	3.0	2.23072	-0.589761
1.0	2.0	0.860674	1.18034
	3.0	-0.410239	1.19659
2.0	2.0	0.278652	1.63933
	3.0	-1.730720	2.08976

reduces with the effect of magnetic field. This implies that the Hartmann number reduces the velocity. Study of Fig. 2c reveals that the influence of the ratio of outer radius to inner radius is to increase the velocity of fluid, because in such situation the annulus space between two cylinders increases, in both cases of heat source and heat sink.

In this section, we have observed the influence of the Hartmann number, ratio of outer radius to inner radius and the heat source/sink parameter on the induced magnetic field. Figs. 3a and 3b show that the induced magnetic field increases and decreases as values of the heat source/sink parameter increase in case of heat source and heat sink respectively due to enhancing the thickness of thermal boundary layer in case of increasing the heat source parameter and reducing in case of increasing the heat sink parameter. The increase in value of the Hartmann number implies that the induced magnetic field decreases since the Lorentz force acts in opposite direction of the induced magnetic field. The ratio of outer radius to inner radius is to increase the induced magnetic field profiles, since the gap between two cylinders increases, in both cases of heat source and heat sink which is shown in Fig. 3c.

In Figs. 4a and 4b, we have analyzed the effect of heat source/sink parameter on the induced current density. It clearly indicates that the induced current density increases with increasing heat source parameter and decreases with increasing heat sink parameter. It is also clear from Figs. 4a and 4b that the induced current density has decreasing tendency with increasing value of the Hartmann number due to the presence

**Table 2** Numerical values of the skin-friction at inner and outer cylinder in non-dimensional form.

$S$	$\lambda$	Ha	$\tau_1$	$\tau_2$	$Q$	$J$	
-2.0	1.8	2.0	0.218179	0.0635563	0.108529	$-7.63278 \times 10^{-17}$	
		3.0	0.216758	0.0643458	0.105685	0.0	
		4.0	0.214941	0.0653552	0.102046	$-2.94903 \times 10^{-17}$	
	2.0	2.0	0.234067	0.0479931	0.159515	0.0	
		3.0	0.231403	0.0493252	0.154008	$-4.44089 \times 10^{-16}$	
		4.0	0.228105	0.0509743	0.147173	0.0	
	3.0	2.0	-0.320533	-0.359025	-3.62186	$-2.22045 \times 10^{-16}$	
		3.0	-0.358803	-0.346268	-3.32340	$8.88178 \times 10^{-16}$	
		4.0	-0.399614	-0.332664	-3.00211	$-2.22045 \times 10^{-16}$	
	-1.0	1.8	2.0	0.243736	0.0827320	0.132299	$2.08167 \times 10^{-17}$
			3.0	0.242484	0.0834277	0.128785	0.0
			4.0	0.240882	0.0843176	0.124290	$-1.73472 \times 10^{-18}$
2.0		2.0	0.286186	0.0849256	0.236942	$-8.32667 \times 10^{-17}$	
		3.0	0.284074	0.0859817	0.228500	$1.11022 \times 10^{-16}$	
		4.0	0.281455	0.0872909	0.218032	0.0	
3.0		2.0	0.189933	-0.0761659	-0.377939	$-3.88578 \times 10^{-16}$	
		3.0	0.169993	-0.0695191	-0.340617	$4.44089 \times 10^{-16}$	
		4.0	0.148673	-0.0624124	-0.300735	$4.45824 \times 10^{-16}$	
1.0		1.8	2.0	0.294850	0.121083	0.179840	$-1.38778 \times 10^{-17}$
			3.0	0.293935	0.121591	0.174986	$2.77556 \times 10^{-17}$
			4.0	0.292763	0.122242	0.168778	$1.73472 \times 10^{-17}$
	2.0	2.0	0.390424	0.158790	0.391796	$-2.77556 \times 10^{-17}$	
		3.0	0.389416	0.159295	0.377485	$5.55112 \times 10^{-17}$	
		4.0	0.388157	0.159924	0.359748	$-2.77556 \times 10^{-17}$	
	3.0	2.0	1.21087	0.489552	6.10990	$-5.55112 \times 10^{-17}$	
		3.0	1.22758	0.483979	5.62494	0.0	
		4.0	1.24525	0.478092	5.10201	$-2.22045 \times 10^{-16}$	
	2.0	1.8	2.0	0.320407	0.140259	0.203611	$-1.38778 \times 10^{-17}$
			3.0	0.319661	0.140673	0.198086	0.0
			4.0	0.318704	0.141205	0.191022	$-4.16334 \times 10^{-17}$
2.0		2.0	0.442544	0.195723	0.469224	$-5.55112 \times 10^{-17}$	
		3.0	0.442087	0.195951	0.451978	0.0	
		4.0	0.441508	0.196241	0.430607	$2.77556 \times 10^{-17}$	
3.0		2.0	1.72133	0.772411	9.35382	$2.77556 \times 10^{-16}$	
		3.0	1.75638	0.760728	8.60772	0.0	
		4.0	1.79353	0.748343	7.80339	$-4.30211 \times 10^{-16}$	

of Lorentz force. Study of Fig. 4c indicates that the induced current density profiles have increasing nature with increasing value of ratio of outer radius to inner radius, due to increment in the annulus space between both the cylinders.

The effects of the heat source/sink parameter and the ratio of outer radius to inner radius on the temperature field are shown in Figs. 5a and 5b. The influence of ratio of outer radius to inner radius is to enhance the temperature field for both heat source and heat sink. It is also observed that an increase in the heat source/sink parameter leads to increase in the temperature profiles, due to reducing the thickness of thermal boundary layer.

The effects of the heat source/sink parameter and the ratio of outer radius to inner radius on the Nusselt number are presented in Table 1. It is observed that the numerical value of the Nusselt number at inner (outer) cylinder decreases (increases) with increasing the heat source/sink parameter in case of heat source and having reverse trend in case of heat sink. This implies that the thermal source has tendency to enhance rate of heat transfer at cylindrical walls whereas thermal sink has reverse effect on it.

Table 2 represents numerical values of the skin-friction at inner surface of outer cylinder and at outer surface of inner cylinder, mass flux and induced current flux of fluid. This is attributed to the fact that the skin-friction at cylindrical walls and mass flux increase and decrease with increasing the heat source/sink parameter in case of heat source and heat sink respectively. The skin-friction and mass flux increase with increasing ratio of outer radius to inner radius in case of heat source but in case of heat sink it increases for  $\lambda \leq 2.0$  and decreases for  $\lambda > 2.0$ . The skin-friction decreases with increasing the Hartmann number at inner and outer cylinders in case of heat sink for any values of ratio of outer radius to inner radius and in case of heat source it decreases for  $\lambda \leq 2.0$  and then increases for  $\lambda > 2.0$ . The mass flux has decreasing tendency with increasing the Hartmann number in case of heat source for any values of ratio of outer radius to inner radius and in case of heat sink it has decreasing tendency with increasing the Hartmann for  $\lambda \leq 2.0$  and increasing tendency for  $\lambda > 2.0$ . The induced current has oscillatory nature with increasing the Hartmann number, heat source/sink parameter and ratio of outer radius to inner radius in both cases of heat source and heat sink.

## 5. Conclusions

In the present investigation, the effects of induced magnetic and heat source/sink on natural convective flow in vertical concentric annuli are carried out. The following conclusions have been drawn from the present analysis:

- The velocity, induced magnetic field and induced current density have decreasing tendency with increase in the value of Hartmann number in both cases of heat source and heat sink.
- The effect of induced magnetic field is to increase the velocity, induced magnetic field and induced current density profiles.
- The effect of heat source/sink parameter is to increase the values of velocity, induced magnetic field, induced current density and temperature field in case of heat source and to decrease all these fields in case of heat sink.

- The ratio of outer radius to inner radius is to increase the velocity, induced magnetic field, induced current density and temperature field in both cases of heat source and heat sink.
- Numerical values of Nusselt number at inner (at outer) cylinder decrease (increases) with increasing heat source/sink parameter in case of heat source and increase (decreases) in case of heat sink.
- Also, the numerical values of skin friction and mass flux at cylindrical walls increase (decrease) with increasing heat source/sink parameter in case of heat source (sink) and in generally they have decreasing tendency with increasing Hartmann number.

## Acknowledgment

One of the authors, Dileep Kumar is thankful to the University Grants Commission, New Delhi for financial assistance in the form of a Fellowship to carry out this work.

## Appendix A

$$\begin{aligned} A_1 &= (A_{10} - A_{11})/2(1 - \lambda^{\text{Ha}}), & A_2 &= (A_{10} + A_{11})/2(1 - \lambda^{-\text{Ha}}), \\ A_3 &= -(A_1 + A_2 + A_5 + A_6S), & A_4 &= -A_9/(4 - \text{Ha}^2), \\ A_5 &= -A_8/(4 - \text{Ha}^2) + 4A_9/(4 - \text{Ha}^2)^2, & A_6 &= 1/4(16 - \text{Ha}^2), \\ A_7 &= \{(A_1 - A_2)/\text{Ha} - (A_4 - 2A_5)/4 + A_6S/4\}, \\ A_8 &= 1 + S/4, & A_9 &= \{-1 + S(\lambda^2 - 1)/4\}/\log \lambda, \\ A_{10} &= A_4\lambda^2 \log \lambda + A_5(\lambda^2 - 1) + A_6(\lambda^4 - 1), \\ A_{11} &= \text{Ha}\{(A_4 - 2A_5)(\lambda^2 - 1) - 2A_4\lambda^2 \log \lambda - A_6S(\lambda^4 - 1)\}/4. \end{aligned}$$

## Appendix B

$$\begin{aligned} B_1 &= (B_{12} - B_{13})/2(1 - \lambda^2), & B_2 &= (B_{12} + B_{13})/2(1 - \lambda^{-2}), \\ B_3 &= -(B_1 + B_2 + B_6S), & B_4 &= -A_9/8, & B_5 &= (-4A_8 + A_9)/16, \\ B_6 &= 1/48, & B_7 &= \{(B_1 - B_2)/2 - B_8 - B_{11}S\}, \\ B_8 &= (B_5 - B_4)/4, & B_9 &= (B_4 - B_5)/2, & B_{10} &= -B_4/2, \\ B_{11} &= -B_6/4, & B_{12} &= \lambda^2 \log \lambda (B_4 \log \lambda + B_5) + B_6S(\lambda^4 - 1), \\ B_{13} &= 2\{B_8(\lambda^2 - 1) + (B_9 + B_{10} \log \lambda)\lambda^2 \log \lambda + B_{11}S(\lambda^4 - 1)\}. \end{aligned}$$

## Appendix C

$$\begin{aligned} C_1 &= (C_{12} - C_{13})/2(1 - \lambda^4), & C_2 &= (C_{12} + C_{13})/2(1 - \lambda^{-4}), \\ C_3 &= -(C_1 + C_2 + C_5), & C_4 &= A_9/12, & C_5 &= (C_9 + 3C_8)/36, \\ C_6 &= 1/32, & C_7 &= \{(C_1 - C_2)/4 - C_8 - C_{10}S\}, \\ C_8 &= (C_4 - C_5)/4, & C_9 &= -C_4/2, & C_{10} &= C_6/16, \\ C_{11} &= -C_6/4, & C_{12} &= C_4\lambda^2 \log \lambda + C_5(\lambda^2 - 1) + C_6S\lambda^4 \log \lambda, \\ C_{13} &= 4\{C_8(\lambda^2 - 1) + C_9\lambda^2 \log \lambda + C_{10}S(\lambda^4 - 1) + C_{11}S\lambda^4 \log \lambda\}. \end{aligned}$$

## References

- [1] M. Couette, Effect of viscous incompressible fluid flow in concentric annuli, *Ann. Chem. Phys.* 21 (6) (1890) 433.
- [2] P. Ramamoorthy, Flow between two concentric rotating cylinders with a radial magnetic field, *Phys. Fluid* 4 (1961) 1444–1445.

- [3] R.K. Jain, K.N. Mehta, Laminar hydromagnetic flow in a rectangular channel with porous walls, *Phys. Fluids* 5 (1962) 1207.
- [4] A. Raptis, A.K. Singh, MHD free convection flow past an accelerated vertical plate, *Int. Commun. Heat Mass Transfer* 10 (1983) 313–321.
- [5] A.J. Chamkha, Hydromagnetic natural convection from an isothermal inclined surface adjacent to a thermally stratified porous medium, *Int. J. Eng. Sci.* 35 (1997) 975–986.
- [6] B.K. Jha, C.A. Apere, Magnetohydrodynamic free convective Couette flow with suction and injection, *J. Heat Transfer* 133 (9) (2011) 12.
- [7] M. Sheikholeslami, M. Gorji-Bandpy, D.D. Ganji, Numerical investigation of MHD effects on  $\text{Al}_2\text{O}_3$ –water nano-fluid flow and heat transfer in a semi annulus enclosure using LBM, *Energy* 60 (2013) 501–510.
- [8] M. Sheikholeslami, S. Abelman, D.D. Ganji, Numerical simulation of MHD nano-fluid flow and heat transfer considering viscous dissipation, *Int. J. Heat Mass Transfer* 79 (2014) 212–222.
- [9] M.M. Hamza, I.G. Usman, A. Sule, Unsteady/steady hydro-magnetic convective flow between two vertical walls in the presence of variable thermal conductivity, *J. Fluids* (2015) 1–9.
- [10] M. Sheikholeslami, M.M. Rashidi, Effect of space dependent magnetic field on free convection of  $\text{Fe}_3\text{O}_4$ –water nano-fluid, *J. Taiwan Inst. Chem. Eng.* 56 (2015) 6–15.
- [11] M. Sheikholeslami, M.M. Rashidi, T. Hayat, D.D. Ganji, Free convection of magnetic nano-fluid considering MFD viscosity effect, *J. Mol. Liq.* 218 (2016) 393–399.
- [12] M. Sheikholeslami, T. Hayat, A. Alsaedi, MHD free convection of  $\text{Al}_2\text{O}_3$ – water nano-fluid considering thermal radiation: a numerical study, *Int. J. Heat Mass Transfer* 96 (2016) 513–524.
- [13] K.L. Arora, R.P. Gupta, Magnetohydrodynamic flow between two rotating coaxial cylinders under radial magnetic field, *Phys. Fluid* 15 (1971) 1146–1148.
- [14] S.K. Singh, B.K. Jha, A.K. Singh, Natural convection in vertical concentric annuli under a radial magnetic field, *Heat Mass Transfer* 32 (1997) 399–401.
- [15] M. Guria, B.K. Das, R.N. Jana, S.K. Ghosh, Effects of wall conductance on MHD fully developed flow with asymmetric heating of the wall, *Int. J. Fluid Mech. Res.* 34 (2007) 521–534.
- [16] R.K. Singh, A.K. Singh, N.C. Sacheti, P. Chandran, On hydromagnetic free convection in the presence of induced magnetic field, *Heat Mass Transfer* 46 (2010) 523–529.
- [17] R.K. Singh, A.K. Singh, Effect of induced magnetic field on natural convection in vertical concentric annuli, *Acta. Mech. Sin.* 28 (2012) 315–323.
- [18] A. Kumar, A.K. Singh, Effect of induced magnetic field on natural convection in vertical concentric annuli heated/cooled asymmetrically, *J. Appl. Fluid Mech.* 6 (2013) 15–26.
- [19] L.J. Crane, Flow past a stretching plate, *ZAMP* 21 (1970) 645–647.
- [20] A.J. Chamkha, H.S. Takhar, G. Nath, Mixed convection flow over a vertical plate with localized heating (cooling), magnetic field and suction (injection), *Heat Mass Transfer* 40 (2004) 835–841.
- [21] P.R. Sharma, G. Singh, Effects of variable thermal conductivity and heat source/sink on MHD flow near a stagnation point on a linearly stretching sheet, *J. Appl. Fluid Mech.* 2 (1) (2009) 13–21.
- [22] K. Bhattacharyya, Effects of radiation and heat source/sink on unsteady MHD boundary layer flow and heat transfer over a shrinking sheet with suction/injection, *Front. Chem. Sci. Eng.* 5 (3) (2011) 376–384.
- [23] B. Lavanya, A.L. Ratnam, Radiation and mass transfer effects on unsteady MHD natural convective flow past a vertical porous plate embedded in a porous medium in a slip flow regime with heat source/sink and Soret effect, *Int. J. Eng. Tech. Res.* 2 (2014).
- [24] P.R. Babu, J.A. Rao, S. Sheri, Radiation effect on MHD heat and mass transfer flow over a shrinking sheet with mass suction, *J. Appl. Fluid Mech.* 7 (4) (2014) 641–650.
- [25] S. Ibrahim, Mohammed, K. Suneetha, Effects of heat generation and thermal radiation on steady MHD flow near a stagnation point on a linear stretching sheet in porous medium and presence of variable thermal conductivity and mass transfer, *J. Comput. Appl. Res. Mech. Eng.* 4 (2015) 133–144.
- [26] D. Kumar, A.K. Singh, Effect of induced magnetic field on natural convection with Newtonian heating/cooling in vertical concentric annuli, *Procedia Eng.* 127 (2015) 568–574.